São José dos Campos - SP
LV SBPO
LV Simpósio Brasileiro de Pesquisa Operacional
São José dos Campos, SP - 6 a 9 de novembro de 2023

Use of multicriteria analysis and map algebra to identify risk areas for multiple health aggravations

Gesiel Rios Lopes, Alexandre C. B. Delbem
Institute of Mathematical and Computer Sciences – University of São Paulo
São Carlos-SP, Brazil
gesielrios@usp.br, acbd@icmc.usp.br

Roberto Fray da Silva
Institute of Advanced Studies – University of São Paulo
São Paulo-SP, Brazil
roberto.fray.silva@gmail.com

Karina Jorge Pelarigo, Mellina Yamamura
Department of Nursing – Federal University of São Carlos
São Carlos-SP, Brazil
karoufscar@hotmail.com, mellina@ufscar.br

Denise Scatolini
Center for Disease Control and Prevention – São Carlos Municipality
São Carlos-SP, Brazil
denise.scatolini@saocarlos.sp.gov.br

ABSTRACT

The COVID-19 pandemic has highlighted the importance of health surveillance actions worldwide, which manage various data sources. Several analyzes can be carried out to qualify health actions and interventions. This work presents a multicriteria spatial model for identifying risk areas for multiple health aggravation, considering population density, disease geographic distribution patterns, and socio-environmental factors. We used the Analytical Hierarchy Process (AHP) method to weigh the degree of importance of each model component and map algebra to combine these components, generating a map with risk areas. A study case was conducted for São Carlos from January 1, 2020, to December 31, 2020, considering multiple aggravations. The data used were: (i) notified and confirmed dengue fever cases; (ii) COVID-19 confirmed cases; (iii) tuberculosis confirmed cases; and (iv) demographic information from the 2010 census. The results showed that the proposed model captures the spatial association for the entire data set. This is critical to characterize the region and the spatial dependence of the variables in neighboring regions. The proposed model integrated maps of multiple aggravations, considering multiple data sources, allowing professionals from different domains to identify high-risk areas more precisely. Additionally, the results from using the proposed method can become a tool for the qualification and direction of health surveillance actions.

KEYWORDS. Decision making. Analytical Hierarchy Process. Map Algebra. Data fusion. Map Visualization

1. Introduction

To establish coherent policies, the territory (or geographical space) is a fundamental part of planning actions to promote and provide comprehensive health care since it is from there that demographic and epidemiological distribution information is obtained involving social, political, cultural, and administrative context Lima et al. [2019]; Melo et al. [2022].

One issue for decision-making in health area is the consistent integration of information from different sources Liu e Zhu [2021]. For example, Health Surveillance activities consider data from patients at different levels of care by healthcare units, transmission vectors, socioeconomic aspects, multiple morbidities (which can generate diagnostic confusion and aggravations), and the resources of the Health System distributed in the city regions of the city.

The decision-making also requires structuring of information with adequate representation for the phenomenon under analysis. The information must, for example, be aggregated according to specific spatial granularity, which may differ among regions of social and epidemiological data and even among data from different epidemics. Time granularity is also important as epidemiological cycles can also differ, in addition to seasonal aspects Lima et al. [2019]; Melo et al. [2022].

Many works in the literature address using Multicriteria Decision Making Methods (MCDM), such as the Analytical Hierarchy Process (AHP), to overcome this challenge. In Ferreira e Silva [2020], the authors use AHP and map algebra to determine the environmental fragility of the Rio Brilhante watershed in Mato Grosso do Sul, Brazil, from the superposition of natural and anthropic factors. The authors use the AHP method to define a set of weights with the level of importance among the variables with the most significant influence on the definition of the basin's environmental fragility from an expert's paired analysis.

Chabuk et al. [2017], use AHP method to define the hierarchical importance of physical and environmental factors that contribute to the potential environmental fragility assessment of the Jequitinhonha river basin, Minas Gerais, Brazil. Another work with a similar proposal is Hongoh et al. [2011], where the authors propose an MCDM-based approach to develop geospatial models and spatially explicit decision support tools for managing vector-borne diseases.

Thus, it is observed that the most relevant works in the literature use subjective MCDM methods Odu [2019] such as the AHP to determine the degree of importance. However, there needs to be more tools for decision-making by health managers who consider, mainly, the potential for multiple health aggravations with possible areas of co-occurrence and demographic and social information. Such possibilities enhance comprehensive care with a view to the quality of life.

In this context, this work aims to propose a spatial model for identifying risk areas through map algebra and the AHP method for the control and prevention of multiple health aggravations, considering population density, patterns of the geographic distribution of diseases, and their relationships with socio-environmental factors, an unusual approach compared to the literature. The results presented by the model should support epidemiological analyzes and the identification of risk areas.

2. Material and methods

2.1. Study area

In this work, we use the methodology of geographic ecological studies, using census tracts [1] of the urban area of the municipality of São Carlos, a medium-sized city in the interior of the state of São Paulo, southeastern Brazil. Located in the central-eastern region of the state (Figure 1), at coordinates 22° 1' 4" South latitude and 47° 53' 27" West latitude, São Carlos has a total area

[1]The census sector is the territorial unit established for cadastral control purposes, formed by a continuous area, located in a single urban or rural area, with size and number of households that allow the survey by a census taker.

of 1,136.907 km^2, average altitude of 856 meters, demographic density of 195.15 inhabitants/km² and resident population of 221,950 inhabitants in 2010. Concerning socioeconomic aspects, the municipality has Gini index of 0.63, human development index (HDI) of 0.805, and gross domestic product of R$ 6,712,498.00 for the same year, 2010.

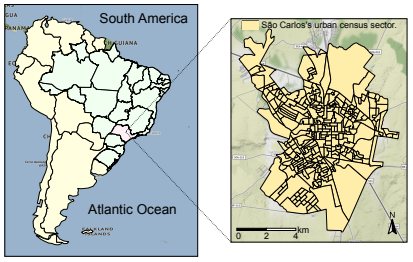

Figure 1: Location of the municipality and urban perimeter of São Carlos – SP.

2.2. Data source

The following data was used in this work: (i) notified and confirmed dengue fever cases from the SINAN-Dengue Notifiable Diseases Information System; (ii) COVID-19 confirmed cases from the SIVEP Influenza health information systems; and (iii) tuberculosis cases registered in the tuberculosis patient control system of the state of São Paulo (TB-WEB). The analysis period was from January 1, 2020, to December 31, 2020, and the data was made available by the city's Epidemiological Surveillance (VIGEP-SC).

For data analysis, cleaning and anonymization were firstly carried out by removing duplicate data, inconsistent dates, and either unwanted or invalid information, in addition to any data related to patients, such as name, telephone number, and date of birth. After this step, all dengue, COVID-19 and tuberculosis cases were georeferenced using Google Maps Geocoding API to obtain the respective geographic coordinates for notified residential addresses. Once the geographic coordinates of all notifications have been determined, aggregation with the urban census sector grid of the municipality of São Carlos was performed using a spatial join function, removing the geolocated data outside the area under study. Figure 3 shows the workflow used to perform this geocoding process. Figure 2 shows the workflow used to perform this geocoding process.

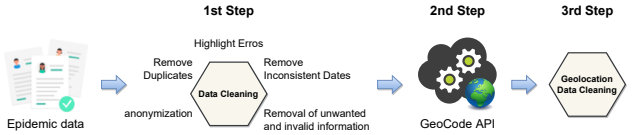

Figure 2: Workflow used to perform the geocoding process.

2.3. Variable selection

A set of thematic maps necessary to model the mapping of critical regions about multiple epidemics was raised, depending on availability data and spatial bases from the opinion of a group of multidisciplinary experts, comprising physicians, epidemiologists, nurses, statisticians and specialists in geoprocessing. Table 1 presents the set of variables used in the modeling.

2.4. Description of Variables

2.4.1. Presence of Health Units

Being the main sites of convergence for infected people who seek health care, health care units are very likely to become vulnerable points from contagion, spread perspective.

Table 1: Variables used in modeling.

Variable	Variable name	Data Source
Presence of Health Units	HUCount	VIGEP-SC
Demographic density	DemoDens	IBGE 2010
Average Residents per HouseHold	MorPDom	IBGE 2010
Percentage of population aged over 60 years	PercPop60	IBGE 2010
Paulista Social Vulnerability Index	IPVS	SEADE SP
Dengue case count	dengueCount	VIGEP-SC
COVID-19 case count	covidCount	VIGEP-SC
Tuberculosis case count	tbCount	VIGEP-SC

Health units were spatialized from their addresses provided by the Health Department of the municipality of São Carlos through address geocoding. These units were classified according to their characteristics, service capacity, and scope. Table 2 presents the classification groups of the health units.

Table 2: Health unit classification groups.

Group	Acronym	Score	Coverage Radius (m)
Family health unit	USF	1	40
Health insurance clinics	CV	2	80
Basic health unit	UBS	3	120
Emergency care unit	UPA	4	160
Hospitals	HOSP	5	200

With the definition of a coverage radius and the spatialized points, a *buffer* layer was generated that is crossed with the layer of census tracts. The *score* for this variable in each sector was calculated by the sum of the *scores* of each health unit whose *buffer* intersected the referred sector. The *score* of this variable for each sector is given by counting the points located within the sector.

2.4.2. Demographic density

The greater the number of individuals in a given region, the greater the probability that individuals will infect each other. In this way, analyzing each sector's demographic density helps identify areas with greater agglomeration capacity.

This analysis used the population database from IBGE demographic census, carried out in 2010 with aggregation at the level of census sector. With the total population aggregated for the sectors, the demographic density in inhabitants per square kilometer was calculated according to the area of each polygon corresponding to the sectors.

Since the city contains almost three hundred sectors, and due to the breadth of these results, we need, in order to be able to rank them and assign them *scores* to represent them in a classification of the variable by intervals. Different data classification methods are described in the literature, Matsumoto et al. [2017] describes several of these methods, highlighting the importance of choosing an adequate method for the desired faithful representation. In this particular study, we used the quantile method to classify data to assign *scores* to them, whose main characteristic is to

form classes with an approximate number of assigned features. Population density values were then sliced into five groups according to their quintiles.

Figure 3(a) shows the histogram of demographic density data, and Figure 3(b) shows the distribution of demographic density in sectors according to these groups. Each group was assigned a score ranging from 1 to 5 points according to the increase in demographic density.

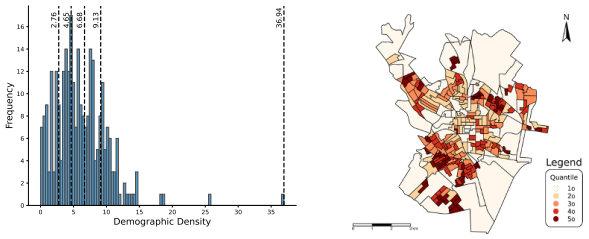

(a) (b)

Figure 3: (a) Histogram of population density data with quintile lines and (b)Choroplectic representation of the distribution of population density.

2.4.3. Average Residents per Household

Analogously to demographic density, within the household, a higher probability of contagion is expected for a greater number of residents. This is also in line with the thought brought to the discussion by health professionals that the number of people sleeping in the same bedroom should be considered.

In this case, IBGE 2010 census database was also used. This data considers the total population in the sector and the respective household count. The same slicing procedure used for the previous variable was adopted for this variable.

Figure 4(a) shows the histogram of data on the average number of residents per household, with break lines adopted for slicing according to quintiles. Figure 4(b) shows the distribution of the average number of residents per household in the sectors according to these groups.

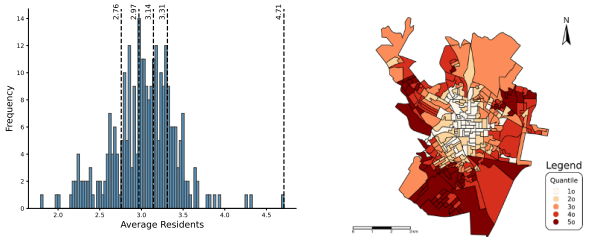

(a) (b)

Figure 4: (a) Histogram of average data for residents per household with quintile lines, and (b) Choroplectic representation of the average distribution of residents per household.

Each group was assigned with a *score* ranging from 1 to 5 points was assigned according to the increase in the average number of residents per household.

2.4.4. percentage of the population aged over 60 years

From the point of view of epidemiological criticality, it is known that age is one of the most relevant risk factors. In order to contemplate this characteristic in the modeling, from the census data, the accumulated population aged over 60 years was accounted for, and the percentage value was calculated in relation to the total for each sector. The same slicing procedure used for both previous variables was adopted in this case.

Figure 5(a) shows the histogram of data on the percentage of the population aged over 60, and Figure 5(b) it is possible to visualize the distribution of the percentage of the population aged over 60 years in the sectors according to these groups.

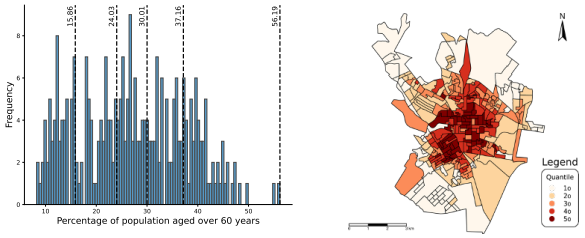

(a) (b)

Figure 5: (a) Histogram of data on the percentage of the population aged over 60 years and (b) Choropleth representation of the distribution of the percentage of the population aged over 60 years.

Each group was assigned a *score* ranging from 1 to 5 points according to the increase in the percentage of the population aged over 60 years.

2.4.5. Paulista Social Vulnerability Index

Knowledge on prior condition of social vulnerability in a region is another relevant factor to be considered when facing the challenges concerning an epidemic, mainly from the point of view of criticality of risks..

Social vulnerability was described with the help of data from "Fundação Sistema Estadual de Análise de Dados (SEADE)", referring to São Paulo Social Vulnerability Index (IPVS) for 2010. This index classifies census sectors based on a combination of demographic and socioeconomic dimensions. It identifies specific factors that deteriorate of living conditions in a community, helping to define priorities for the care of the most vulnerable population Alves [2020].

IPVS incorporates the following indicators: number of inhabitants; average nominal income of households; the average age of heads of households; percentage of heads of households under 30 years of age, female heads of households under 30 years of age, and the share of children under six years of age, over the denominator of the total inhabitants of each of these segments Alves [2020], characterizing the census sectors in seven groups: Group 1–extremely low vulnerability; Group 2–very low vulnerability; Group 3–low vulnerability; Group 4–medium vulnerability; Group 5–high vulnerability; Group 6–very high vulnerability and Group 7–very high vulnerability. Figure 8 shows the choropleth representation of the IPVS distribution for São Carlos-SP.

IPVS consists of a typology of situations of exposure to vulnerability, adding to the income indicators, others referring to the family life cycle and schooling in the intra-urban space. Indeed, among the questions investigated by the 2010 Demographic Census in its basic questionnaire, in addition to socioeconomic variables (income and literacy status), those related to the family life cycle (presence of young children, age, and gender of the head of the household) were selected.

The *scores* for each sector received values from 1 to 6 ranging from very low vulnerability to high or very high vulnerability. In Figure 6, it is possible to visualize the distribution of IPVS in the sectors.

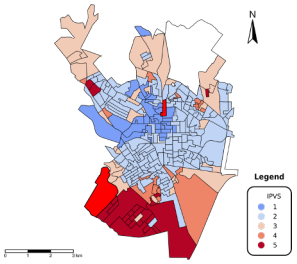

Figure 6: Choropleth representation of the IPVS distribution for São Carlos-SP.

2.4.6. Case Count

The previous existence of cases in a particular region puts it under an even more severe risk condition. The greater the number of these cases, the worse the condition of the region.

Counting by census tracts was done using a *join spatial* function, which crosses the layers. In this case, a radius of coverage was not considered since quarantine is imposed on people who test positive when returning home.

Figure 7(a), the spatial distribution of confirmed dengue cases in 2020 can be seen. Figure 7(b), the spatial distribution of cases is presented of COVID-19 in 2020, and in Figure 7(c), we have the spatial distribution of tuberculosis cases in 2020.

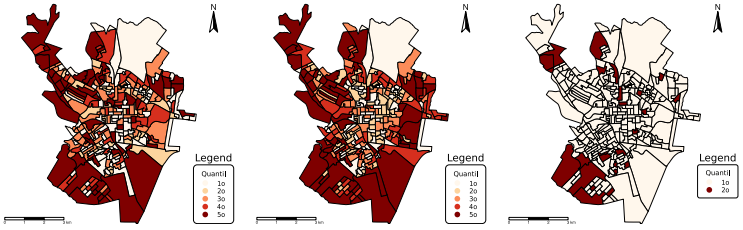

(a) (b) (c)

Figure 7: (a) Choroplectic representation of the spatial distribution of notified cases of Dengue in 2020, (b) Choroplectic representation of the spatial distribution of notified cases of COVID-19 in 2020 and (c) Choroplectic representation of the spatial distribution of notified cases of tuberculosis in 2020.

The *scores* of each sector is the case count.

2.5. Model Definition

Accordingly, the task of understanding and mapping the risks, problems, and difficulties in coping with an epidemic is complex and involves different variables with diverse characteristics and often from diffuse sources. It is necessary to choose alternatives and establish a rational model for combining the data. In this context, geoprocessing can offer support tools for decision-making that help the specialist in this task.

The fundamental concept of the various decision-making models is that of rationality. According to this principle, individuals and organizations follow the behavior of choosing between alternatives based on objective judgment criteria, whose foundation will be to satisfy a pre-established desired level.

When different factors contribute to the decision, it is necessary to determine their relative contribution. To address this problem Saaty [1978] proposed a selection technique based on pairwise comparison logic. In this procedure, the different factors that influence decision-making are compared two-by-two, and a criterion of relative importance is assigned to the relationship between these factors according to a predefined scale. This technique is commonly used in geoprocessing and is known as Analytic Hierarchy Process (AHP).

To determine the relative contribution of each model variable, it was first decided to classify them into three groups according to demographic, social, and epidemiological aspects. Figure 8 presents the variables classified according to these aspects.

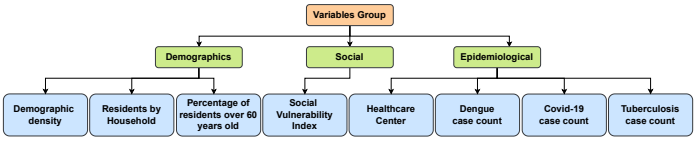

Figure 8: Classification of variables.

Next, a pairwise comparison was performed between groups and variables using the fundamental scale of the AHP method Saaty [1978] to assess the contribution and relative importance between groups and variables. Table 3 presents the paired comparison matrix and the respective weights of each group. Table 4 presents the paired comparison matrix and the respective weights for each variable.

Table 3: Pairwise comparison matrix for groups.

Group	Pairwise Matrix	A	B	C	Weights
Demographics	A	1.00	3.00	0.50	0.31
Social	B	0.33	1.00	0.20	0.11
Epidemiological	C	2.00	5.00	1.00	0.58

Table 4: Pairwise comparison matrix for variables.

Group	Variable		A	B	C	D	Weights
Demographics	DemoDens	A	1.00	0.50	0.20	-	0.12
	MorPDom	B	2.00	1.00	0.33	-	0.23
	PercPop60	C	5.00	3.00	1.00	-	0.65
Social	IPVS	A	1.00	-	-	-	1.00
Epidemiological	HUCount	A	1.00	2.00	2.00	2.00	0.33
	dengueCount	B	0.50	1.00	6.00	6.00	0.46
	covidCount	C	0.50	0.17	1.00	6.00	0.15
	tbCount	D	0.50	0.17	0.17	1.00	0.06

The Consistency Ratio (CR) was calculated to validate pairwise comparisons between groups and variables. The Consistency Ratio for groups of variables and demographic variables was 0.005 ($CR_{group} = CR_{var\_dem}0.005$), while for epidemiological variables, it was 0.21 ($CR_{var\_epi} =$

0.21). Thus, the value of CR ≤ 0.01 Saaty e Vergas [1992] shows that the relative priority values are consistent.

From these results, we have that the group of epidemiological variables appears with the highest level of influence for determining critical areas. Concerning the demographic variables, the variable that represents the percentage of the population over 60 years of age appears to have the highest level of influence concerning the other variables of the same group. This occurred because people in this age group have more significant mobility difficulties and are more susceptible to lung diseases.

For the epidemiological variables, the variable with the most significant influence is the variable that represents the number of dengue cases. This importance is because a vector transmits this condition, and some symptoms are confused with those of other diseases Zhang et al. [2023]. In Figure 9, we can visualize the final composition of the weights for the complete set of variables.

With the definition of the weight of each variable in the model, we calculate a global *score* by crossing the different layers that represent each variable weighted by the respective weights using a weighted linear combination (WLC), expressed by the Equation 1, where the final suitability thematic layer is derived by multiplying each thematic layer by its relative weight followed by the sum of the results.

$$GS = \begin{array}{rcl} 0.31 & \times & \begin{pmatrix} 0.12 \times DemoDens + 0.23 \times MorPDom + \\ 0.65 \times PercPop60 \end{pmatrix} + \\ 0.11 & \times & (1.00 \times IPVS) + \\ 0.58 & \times & \begin{pmatrix} 0.33 \times HUCount + 0.46 \times dengueCount + \\ 0.15 \times covidCount + 0.06 \times tbCount \end{pmatrix} \end{array} \quad (1)$$

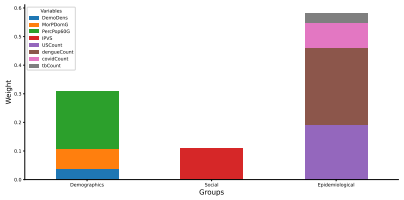

Figure 9: Final composition of the weights.

3. Results and Discussion

From the calculated global *scores* data, the first analysis was conducted to verify its descriptive statistics. These are shown in Figure 10(a).

The global *scores* values were then sliced into five classes according to their natural break values. In this case, the classification method adopted has the characteristic of similar grouping values and maximizing differences between classes, with established limits where there are considerable differences between data values. Thus, this method represents the natural scaling of the data series, grouping them according to Matsumoto et al. [2017] similarity. Figure 10(b) presents the classification of census tracts in relation to the model's global *scores*.

To ensure that the modeling represents the phenomenon from a spatial point of view and thus validate the mapping in question, one of the necessary aspects that we have to answer is whether the event under study and the factors related to it have a spatially conditioned distribution, the spatial autocorrelation was calculated using the Global and Local Moran indicators Moran [1950]

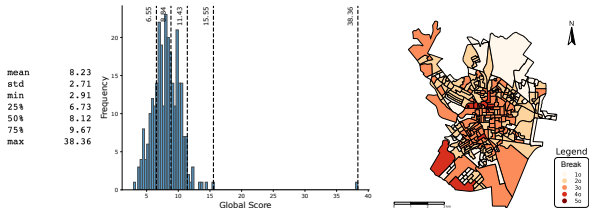

(a) (b)

Figure 10: (a) Descriptive Statistics of the Global Score. and (b) Classification of census sectors in relation to global scores.

considering only the first neighborhood level. The Global Moran indicator was used as a test whose null hypothesis is data independence. The global Moran index is given by Equation 2.

$$I = \frac{\sum_{i=1}^{n}\sum_{j=1}^{n} w_{ij}(z_i - \bar{z})(z_i - \bar{z})}{\sum_{i=1}^{n}(z_i - \bar{z})^2} \tag{2}$$

where n is the number of areas, z_i is the value of the attribute considered in the area i, z is the average of the assigned values in the study region, and w_{ij} the elements from the normalized spatial proximity matrix Moran [1950]

In this case, we have to use spatial statistics, particularly the study of spatial dependence, to demonstrate how values correlate with space and whether and how they depend on values of the same variable in neighboring regions.

The global score values of each sector were used to calculate Moran's I. In Figure 11(a), it is possible to see the result of the test. Given the Moran's I of 0.33, there is less than a 1% probability that this clustering pattern could be a random result. Thus, the spatial distribution of high or low values in the data set is more spatially clustered than expected if the underlying spatial processes were random.

Global indicators such as Moran's I provide a single value to measure spatial association for the entire dataset, which helps characterize the entire region. Thus, we can reject the null hypothesis, but we still cannot significantly analyze the pattern of the clusters Monteiro et al. [2004].

Using the centroids of the census tracts as a starting point, we can vary the neighborhood distance to other centroids to calculate Moran I and thus analyze how spatial dependence is changing as a function of this distance. For this, we analyzed the distances between the centroids pair by pair and found that the minimum distance found was around 130 meters and the maximum around 1600 meters, with an average distance of around 300 meters. This way, Moran's I was calculated for distances every 150 meters starting from 300 meters in 30 intervals. In Figure 11(b), we present the graph of *z-score* variation as a function of the distance. The peaks reflect the distances at which the spatial processes that promote clustering are most pronounced. The color of each point on the graph corresponds to the statistical significance of the *z-score* values.

Finally, we can build a thematic map of the modeling performed. Figure 12 presents the final map of the modeling performed.

From the modeled thematic map, it is possible to observe that we have two critical areas, the central and southern regions of the municipality. The criticality of the central region was because it is the region of the municipality with the highest concentration of people over 60 years old, see Figure 5(b), and the variable considered most greater weight among the demographic variables. Concerning the southern region, there is a large number of census sectors with IPVS 5, see Figure 6,

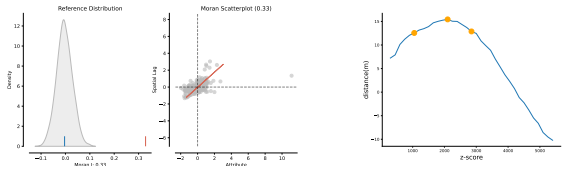

(a) (b)

Figure 11: (a) Moran's I test result and (b) Special autocorrelation as a function of distance.

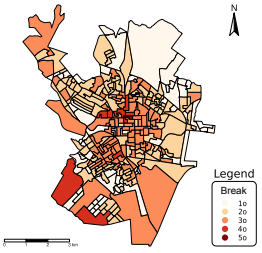

Figure 12: Modeling thematic map.

a region with high social vulnerability, in addition to being the region of the municipality with the highest greater concentration of the conditions considered, see Figure 7, evidencing the model's ability to capture these annuities.

As a limitation of this research, it is highlighted that the identified results cannot be interpreted at the individual level in ecological studies. In addition, individuals can contract the disease in locations other than where they live, highlighting the importance of longitudinal and prospective studies. Furthermore, acquiring information through secondary data raises the possibility of underreporting in low-risk areas and errors regarding the address of the cases, which may generate some bias in the results of this investigation and its analysis.

4. Conclusion and Future Works

Decision makers require methods and interfaces that allow them to take various types of data at different time and space scales, visually compare the results, and also require a dashboard summarizing the main estimates found. In this context, this work presented the definition of a model of integration of maps of multiple health aggravations through map algebras and multicriteria analysis, integrating multiple sources of data, providing professionals from different areas to identify with more precision areas of high risk, being a tool to help epidemiological surveillance in priority intervention areas more effectively.

As future work, it is intended to carry out new studies with analytical designs capable of verifying, with greater reliability, possible associations between the areas of greater risk for illness due to multiple health aggravations, other variables of socioeconomic factors and characteristics of health services, in addition to analyzes space-time of diseases.

Acknowledgments

The authors of this work would like to thank the CAPES (PROEX), CNPQ (grant #312605 /2018-8), Center for Artificial Intelligence (C4AI-USP) and the support from the São Paulo Research Foundation (FAPESP grant #2019/07665-4, #2020/16578-5) and from the IBM Corporation. We would like also to thank the CEPID-CeMEAI/ICMC-USP (CEPID, FAPESP grant #2013/07375-0). We also thank ICMC-USP and LCR for offering the necessary infrastructure for this study.

References

Alves, J. D. G. (2020). O índice paulista de vulnerabilidade social (ipvs) como ferramenta para promoção políticas públicas: aplicação do índice no município de piracicaba–são paulo. *Anais*, p. 1–6.

Chabuk, A., Al-Ansari, N., Hussain, H. M., Knutsson, S., Pusch, R., e Laue, J. (2017). Combining gis applications and method of multi-criteria decision-making (ahp) for landfill siting in al-hashimiyah qadhaa, babylon, iraq. *Sustainability*, 9(11):1932.

Ferreira, P. S. e Silva, C. A. d. (2020). O método ahp e a álgebra de mapas para determinar a fragilidade ambiental da bacia hidrográfica do rio brilhante (mato grosso do sul/brasil), proposições para a gestão do território. *Confins. Revue franco-brésilienne de géographie/Revista franco-brasilera de geografia*, (46).

Hongoh, V., Hoen, A. G., Aenishaenslin, C., Waaub, J.-P., Bélanger, D., e Michel, P. (2011). Spatially explicit multi-criteria decision analysis for managing vector-borne diseases. *International Journal of Health Geographics*, 10(1):1–9.

Lima, L. M. M. d., Melo, A. C. O. d., Vianna, R. P. d. T., e Moraes, R. M. d. (2019). Análise espacial das anomalias congênitas do sistema nervoso. *Cadernos Saúde Coletiva*, 27:257–263.

Liu, W. e Zhu, J. (2021). A multistage decision-making method for multi-source information with shapley optimization based on normal cloud models. *Applied Soft Computing*, 111:107716.

Matsumoto, P. S. S., da Castro Catão, R., e Guimarães, R. B. (2017). Mentiras com mapas na geografia da saúde: métodos de classificação e o caso da base de dados de lva do sinan e do cve. *Hygeia: Revista Brasileira de Geografia Medica e da Saude*, 13(26):211.

Melo, A. C. O. d., Melo, J. C. d. S., e Moraes, R. (2022). Epidemiologia espacial e a detecção de aglomerados espaciais do dengue na paraíba: uma comparação entre os métodos scan flexível e scan circular. *Cadernos Saúde Coletiva*, 30:561–571.

Monteiro, A. M. V., Câmara, G., Carvalho, M., e Druck, S. (2004). Análise espacial de dados geográficos. *Brasília: Embrapa*.

Moran, P. A. (1950). Notes on continuous stochastic phenomena. *Biometrika*, 37(1/2):17–23.

Odu, G. (2019). Weighting methods for multi-criteria decision making technique. *Journal of Applied Sciences and Environmental Management*, 23(8):1449–1457.

Saaty, T. L. (1978). Modeling unstructured decision problems—the theory of analytical hierarchies. *Mathematics and computers in simulation*, 20(3):147–158.

Saaty, T. L. e Vergas, L. (1992). Multicriteria decision making: the analytical hierarchical process. *RWS, Pittsburg. 125p*.

Zhang, B., Zhang, Q.-Q., Cai, Y.-Y., Yan, X.-T., Zhai, Y.-Q., Guo, Z., e Ying, G.-G. (2023). Environmental emissions and pollution characteristics of mosquitocides for the control of dengue fever in a typical urban area. *Science of The Total Environment*, p. 161513.